Towards a Polydisperse Packed Bed Filtration Model as a Surrogate Model for Particulate Filters

By Matthias Bonarens[1,2], Robert Greiner[1], Martin Votsmeier[1,2], and David Vidal[3,4]*

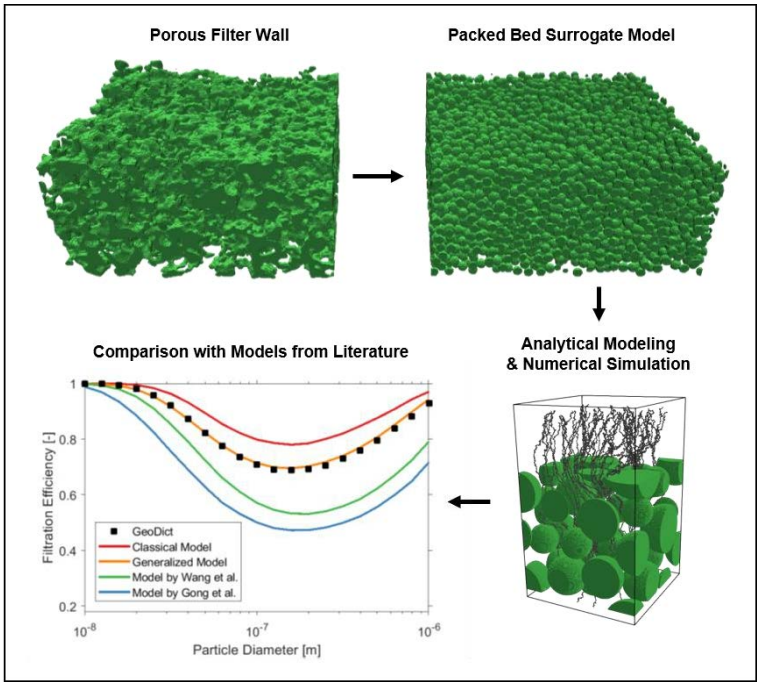

Abstract

Monodisperse packed beds have long been used as surrogate models to predict the filtration performance of particulate filters using analytical methods. In recent years, however, polydisperse packed beds have received special attention as they have the potential to better represent the microstructure of porous filter walls. In this paper, an analytical model for the filtration performance of clean polydisperse packed beds is derived based on the well-proven classical packed bed filtration theory. Predictions of the newly developed model were compared to the results of numerical simulations of the filtration performance of two polydisperse packed beds. The proposed filtration model was in considerably better agreement with the simulations than previous analytical models.

Keywords: GPF, DPF, Particulate Filters, Filtration Efficiency, Polydisperse Packed Bed, Reduced-order Model

[1] Umicore AG & Co. KG, Rodenbacher Chaussee 4, 63457 Hanau, Germany
[2] Technische Universität Darmstadt, Ernst-Berl-Institut für Technische und Makromolekulare Chemie, Alarich-Weiss-Straße 8, 64287, Darmstadt, Germany
[3] Research Center for Industrial Flow Processes (URPEI), Department of Chemical Engineering, Polytechnique Montréal, Montréal, QC, Canada H3C 3A7
[4] Department of Mechanical Engineering, Polytechnique Montréal, Montréal, QC, Canada H3C 3A7

*Corresponding Author

1 Introduction

The formation of soot particles in diesel engines cannot be reduced to an extent that complies with the legal limits for particulate emissions, making after-treatment of their exhaust gas inevitable. (Koltsakis, 2012) To reduce the particulate load released into the environment, diesel vehicles have long been equipped with particulate filters in which the particulate matter is physically separated. (Guan, 2015; Votsmeier, 2009) Given increasingly stringent regulations for all types of internal combustion engines, particulate filters have begun to find broad application for gasoline engines as well, especially for gasoline direct-injection engines. (Joshi, 2018)

The most common type of particulate filters are wall-flow filters in which the particle-laden exhaust is forced to flow through the thin walls of a porous monolith, trapping soot particles in the filter wall due to deep-bed filtration. (Guan, 2015; Votsmeier, 2009; Joshi, 2018) Particulate filters thus accumulate considerable amounts of particulate matter and require regular regeneration by oxidation of the deposited soot. (Guan, 2015; Joshi, 2018; Konstandopoulos, 2000) However, as modern gasoline particulate filters are continuously regenerated due to high operating temperatures, they rarely contain high particle loads. (Adam, 2020) This is why a better understanding of the filtration characteristics of clean particulate filters and the corresponding modelling approaches are of great interest. Clean in this context means that soot particles have not accumulated within the filter to a significant extent. (Logan, 1995)

With the advent of numerical methods such as the lattice Boltzmann method and the finite difference or volume method, which are particularly well suited to flows in porous media due to the ease of discretizing the pore space, detailed investigations of filtration processes within complex filter structures have become feasible. In the last decade, numerous simulation studies investigating various types of filters using custom (Long, 2009; Rebaï, 2011; Matte-Deschênes, 2016; Belot, 2020; Belot, 2021), commercial (e.g., GeoDict® (Gervais, 2015; Azimian, 2017; Belot, 2020)), or open-source (e.g., OpenFOAM (Plachá, 2020)) codes have been conducted, and a good level of success in predicting the flow field and capture efficiency has been achieved using a Langevin solver. Despite their good capabilities for fundamental investigations, numerical simulations are unable to render real-time solutions. A reduced-order model that can provide a good estimate in near real-time is thus required for optimization and control purposes.

Porous filter walls made of cordierite or silicon carbide are complex and irregular structures, as illustrated in Figure 1. A reduced-order surrogate filter model would thus be of great value to facilitate the computation of their filtration characteristics using analytical methods. A packed bed of randomly distributed spherical collector bodies is a surrogate model that has been used in numerous studies. (Konstandopoulos, 1989; Gong, 2015b; Wang, 2020; Walter, 2020; Gong, 2018) Its composition must be adjusted such that it matches the real structure in its essential properties as closely as possible. The classical packed bed filtration theory, first systematically applied to particulate filters by Konstandopoulos et al. (Konstandopoulos, 1989), employs a monodisperse packed bed as a surrogate filter model. As can be seen in Figure 1, however, a monodisperse packed bed cannot fully capture the inhomogeneous microstructure of particulate filters, which actually has a significant impact on their filtration performance. (Viswanathan, 2021) When Gong et al. (Gong, 2015b) proposed polydisperse sphere packed beds as surrogate models it was a major step toward a more realistic modelling approach.

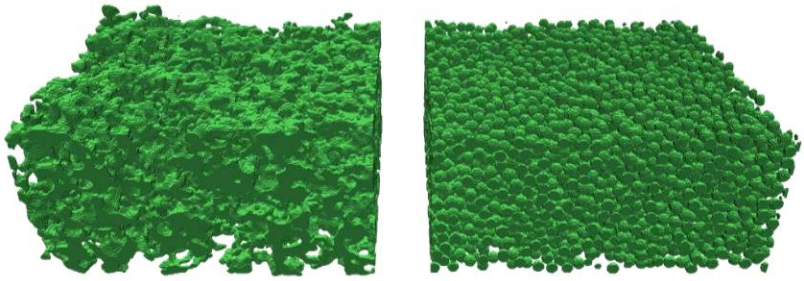

Figure 1: Sections of a gasoline particulate filter wall obtained from computed tomography (Greiner, 2019) *(left) and a monodisperse packed bed as a possible surrogate filter model (right).*

Gong et al. proposed determining the composition of a polydisperse sphere packed bed that is representative of a particular particulate filter based on an analysis of its pore space volume using mercury intrusion porosimetry (MIP). This proposal was adopted in a number of studies (Wang, 2020; Walter, 2020; Gong, 2018), despite several known assumptions and limitations of MIP that could bias associated analyses (e.g., the cylindrical pore shape assumption and the so-called ink-bottle effect that causes a tendency to overestimate the smaller pore population (Diamond, 2000; Moro, 2002)).

Once the composition of a packed bed representative of the filter wall being investigated has been determined, its filtration properties can be modelled. The filtration performance of a packed bed relies on the deposition of particles on the collector bodies that make it up. It is thus necessary to develop a model capable of predicting the filtration characteristics of polydisperse packed beds from those of the collectors, i.e., the spheres they contain. Typically, such theorical approaches assume that the filtration efficiency of a packed bed can be obtained by summing the filtration efficiencies of all its collector bodies. (Gutfinger, 1979) As Gutfinger et al. (Gutfinger, 1979) pointed out, they can therefore be subdivided into the prediction of the filtration properties of the individual collector bodies and the subsequent determination of the filtration performance of the packed bed as a whole. While the filtration characteristics of single-collectors have been subject to extensive research (Gutfinger, 1979; Lee, 1979; Otani, 1989), analytical correlations that use them to predict the filtration performance of polydisperse sphere packed beds are a more recent field of research. To the knowledge of the authors, only two such models have been published so far, both in the context of particulate filters.

Gong et al. (Gong, 2015b) extended a cell model approach for monodisperse packed beds that links the total filtration efficiency of a polydisperse packed bed to a velocity-weighted average of the capture efficiencies of individual monodisperse packed beds of collector diameters corresponding to those contained in the polydisperse packed bed under study, such that:

$$E_{Gong} = \frac{\int_{d_{ci}} PDF(d_{ci})\, U_i\, E_i\, \mathrm{d}d_{ci}}{\int_{d_{ci}} PDF(d_{ci})\, U_i\, \mathrm{d}d_{ci}} = \frac{\int_{d_{ci}} pdf(d_{ci})\, U_i\, E_i\, d_{ci}^3\, \mathrm{d}d_{ci}}{\int_{d_{ci}} pdf(d_{ci})\, U_i\, d_{ci}^3\, \mathrm{d}d_{ci}} \qquad \textit{Eq. 1}$$

In this equation, $E_{Gong} = E_{Gong}(d_\mathrm{p})$ refers to the total filtration efficiency of the polydisperse packed bed considered that depends on the particle size d_p of the aerosol to be captured. $PDF(d_{ci})$ and $pdf(d_{ci})$, respectively, are the normalized volume- and number-based probability density functions of the collector diameters within the polydisperse packed bed (with $PDF(d_{ci})$ derived from MIP by Gong et al.). Furthermore,

$E_i = E_i(d_{ci}, d_p)$ is the filtration efficiency of aerosol particles of diameter d_p achieved by a bed packed with monodisperse collectors of size d_{ci} that has the same porosity ϵ and thickness w as the polydisperse packed bed. This is given by the classical packed bed filtration model that is based on the single-collector theory (Logan, 1995; Konstandopoulos, 1989), a well-known extension of the single-fiber theory used for fibrous filters: (Spurny, 1998; Hinds, 1999)

$$E_i = 1 - \exp\left[-\frac{3}{2}\frac{(1-\varepsilon)\,w}{\varepsilon}\frac{\eta_i}{d_{ci}}\right] \qquad \textit{Eq. 2}$$

In Eq. 2, $\eta_i = \eta_i(d_{ci}, d_p)$ is the efficiency of a single-collector of diameter d_{ci} that can be estimated from the superimposed contributions of existing correlations for Brownian diffusion (η_{Di}), direct interception (η_{Ri}), and inertial impaction (η_{Ii}) capture mechanisms that all depend strongly and differently on d_{ci} and d_p. (Spurny, 1998; Hinds, 1999) Lastly, U_i in Eq. 1 is the collector size-dependent superficial velocity at which the gas flow approaches the individual monodisperse packed beds. According to Gong et al., this is given by Eq. 3, in which $\overline{U}$ represents the superficial velocity obtained across the polydisperse packed bed at a given pressure drop.

$$U_i = \frac{d_{ci}^2}{\int_{d_{ci}} PDF(d_{ci})\ d_{ci}^2\,\mathrm{d}d_{ci}}\overline{U} \approx \frac{d_{"c"\,i}^2}{\sum_i PDF(d_{ci})\ d_{ci}^2}\overline{U} \qquad \textit{Eq. 3}$$

Several theoretical underpinnings of Eq. 1 may be questioned, most prominently the approach of relating the filtration efficiency of a polydisperse packed bed to those of several isolated monodisperse packed beds. Gong et al. validated their model against experiments using various operating conditions and reported relatively good agreement in the diffusion-dominated capture regime, while a tendency to overpredict filtration efficiency was observed in the interception-dominated capture regime. However, this validation study was based on MIP, which entails several shortcomings as discussed above. It also involved fitted parameters, namely the collector size distribution of the filters being examined for which no experimental data was available as well as an interception length. All these reasons may raise reasonable doubts about the proposed model.

In fact, Wang et al. (Wang, 2020) recently revised the previous model such that the overall filtration efficiency of a polydisperse packed bed is no longer calculated as a velocity-weighted average of capture efficiencies of individual monodisperse packed beds but from a velocity-weighted average of the single-collector efficiencies of all collector bodies contained in the polydisperse packed bed being studied. Hence, their formulation is more in line with the original single-collector theory:

$$\begin{aligned} E_{Wang} &= 1 - \exp\left[-\frac{3}{2}\frac{(1-\varepsilon)\,w}{\varepsilon}\int_{d_{ci}}\left(\frac{U_i\,PDF(d_{ci})}{\overline{U}}\frac{\eta_i}{d_{ci}}\right)\mathrm{d}d_{ci}\right] \\ &\approx 1 - \exp\left[-\frac{3}{2}\frac{(1-\varepsilon)\,w}{\varepsilon}\sum_i\left(\frac{U_i\,PDF(d_{ci})}{\overline{U}}\frac{\eta_i}{d_{ci}}\right)\right] \end{aligned} \qquad \textit{Eq. 4}$$

Wang et al. also performed an experimental validation study in which only the capture mechanisms of diffusion and direct interception were considered. Both were accounted for using analytical correlations, but each was preceded by a coefficient to be calibrated from experimental data, which again introduced two degrees of

freedom. Although these might improve the predictive ability of the model, which is quite good compared to experimental data from four different filters and various operating conditions, they actually needed to be calibrated for each material due to the distinctive relationship between the pore space geometry of the material and the MIP measurements. The authors suggested that this calibration can be interpreted as a means of correcting for the distortion of collector size distributions induced by MIP. However, it is also conceivable that the theoretical approach on which the model is based has a potential for optimization.

Inspired by the cell model developed by Kuwabara (Kuwabara, 1959) to investigate the flow around a single-collector in a field of random packed beds, Wang et al. built their filtration model on an idealized cell model in which every collector is situated in the center of a spherical cell. As each cell is to have the same porosity as the packed bed being examined, its size increases with the collector diameter, as does the velocity at which the exhaust gas flows through the cell. To account for this effect, Wang et al. introduced the diameter-dependent velocity term into their filtration equation that ascribes a much greater influence on the overall filtration effect of polydisperse packed beds to large collectors. However, the cell model suggested must be regarded as a simplified approximation that is accompanied by contradictions. First, there is no minimum distance between collectors in a randomly arranged packed bed, so that two collector bodies may be closer together than the cell model implies. Second, even with the most compact arrangement, a void remains between the spherical cells that has no physical interpretation. For these reasons, the conclusions drawn from the cell model suggested are not fully transferable to packed beds and should be considered with caution. As the spatial distribution of the collectors is random and not subject to any regularity, it can readily be argued that the distances between the collector bodies of a packed bed do not depend on their diameter. For these reasons, the actual validity of the proposed model for predicting the collection efficiency of a polydisperse packed bed can be questioned.

The present paper is intended to contribute to the further development of analytical approaches using polydisperse sphere packed beds as a surrogate model for clean particulate filters. More specifically, a new analytical model will be derived from first principles. Together with the filtration models proposed by Gong et al. and Wang et al., this new model will be compared to simulation results obtained using GeoDict® in order to determine the polydisperse packed bed filtration model that agrees best with the simulations.

The remainder of this paper is thus organized as follows. In Section 2, a third possible filtration model is carefully derived from a mass balance over a control volume of a polydisperse packed bed. In Section 3, the methodology used for the comparison of the predictions from all the proposed analytical models with GeoDict® simulation results is described in detail. The outcome of this comparison is presented in Section 4. Lastly, in Section 5, concluding remarks are provided and future opportunities for expanding the use of the most accurate polydisperse packed bed filtration model as a reduced-order surrogate model for particulate filters are briefly discussed.

2 Generalized Packed Bed Filtration Theory

To quantify the filtration performance of a clean filter medium, the filtration efficiency E has proven to be a suitable measure. It is defined as the fraction of incoming particles captured in the filter, such that: (Konstandopoulos, 1989)

$$E = 1 - \frac{\phi_{\text{out}}}{\phi_{\text{in}}} \qquad \textit{Eq. 5}$$

In order to compute the filtration efficiency, the ratio of the number of particles leaving and entering the packed bed per unit time, $\phi_{\text{out}}/\phi_{\text{in}}$, must be known. This can be determined by means of a particle mass balance over a control volume of the packed bed being investigated, as shown in Figure 2.

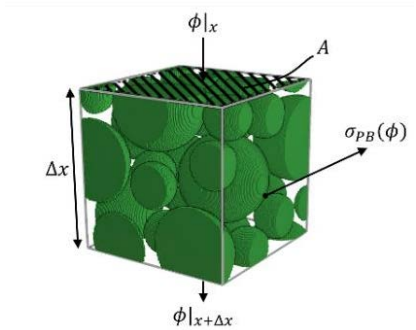

Figure 2: Mass balance over a control volume of the packed bed.

When a particle-laden exhaust gas passes through the element, a certain number of particles adhere to the collector surfaces, reducing the number of particles remaining in the flow. Other effects that affect the particle count, such as agglomeration and particle re-entrainment after capture, are neglected. (Logan, 1995) Since the filtration performance of clean beds are modelled, the accumulation of particles on collector surfaces and the resulting filter clogging are not considered. Thus, the rate at which particles are removed from the exhaust gas as it flows through the packed bed element (PB) can be expressed by a sink term, σ_{PB}. It follows from the particle mass balance that the number of particles escaping from the element per unit time, $\phi|_{\text{x}+\Delta\text{x}}$, corresponds to the rate of incoming particles, $\phi|_{\text{x}}$, reduced by the particles deposited per unit time so that:

$$\phi|_{\text{x}+\Delta\text{x}} = \phi|_{\text{x}} - \sigma_{\text{PB}} \qquad \textit{Eq. 6}$$

Before the filtration efficiency can be determined from this mass balance, a relation between the sink term and the properties of the collectors within the element has to be found. The classical packed bed filtration theory provides such an equation only for monodisperse packed beds. However, the theoretical approach underlying the widely accepted classical model can be generalized to also cover polydisperse packed beds. For this purpose, it is helpful to first briefly revisit the classical filtration theory based on the concise description given by Logan et al. (Logan, 1995)

2.1 Classical Packed Bed Filtration Model

The filtration properties of packed beds can be attributed to the deposition of particles on the surface of the collectors of which it is composed. Since all collectors in a monodisperse packed bed equal each other, the rate of particles collected in an element, σ_{PB}, corresponds to the rate at which particles adhere to a single-collector body (SC), σ_{SC}, multiplied by the number of collector bodies, N_{SC}: (Logan, 1995)

$$\sigma_{\text{PB}} = \sigma_{\text{SC}} \cdot N_{\text{SC}} \qquad \textit{Eq. 7}$$

The deposition rate σ_{SC} equals the rate at which particles impinge on a single-collector multiplied by the probability that the particles will actually adhere to it, which is often called the sticking coefficient α (with 0 ≤ α

≤ 1). The particle impingement rate can be related to the number of particles approaching a collector per unit time, ϕ_{SC}, multiplied by the single-collector efficiency, η, that gives the fraction of approaching particles that actually strike the collector, such that: (Logan, 1995)

$$\sigma_{\mathrm{SC}} = \alpha \cdot \eta \cdot \phi_{\mathrm{SC}} \qquad \textit{Eq. 8}$$

The rate of particles approaching a single-collector is defined as the rate at which particles pass through an area corresponding to the projected area of the collector sphere. Within the packed bed, the particle flux depends on its porosity, ε, and is given by $\phi/(A \cdot \varepsilon)$. The rate of approaching particles is thus obtained by multiplying the particle flux with the projected area of a collector body, which only depends on its diameter d_{c} so that: (Logan, 1995)

$$\sigma_{\mathrm{SC}} = \alpha \cdot \eta \cdot \frac{\phi}{A \cdot \varepsilon} \cdot \frac{\pi \cdot {d_{\mathrm{c}}}^2}{4} \qquad \textit{Eq. 9}$$

The total number of collectors in the control volume can then be calculated from geometrical considerations assuming that the entire solid volume fraction of the element, $(1-\varepsilon) \cdot A \cdot \Delta x$, is occupied by collectors: (Logan, 1995)

$$N_{\mathrm{SC}} = \frac{6 \cdot (1-\varepsilon) \cdot A \cdot \Delta x}{\pi \cdot {d_{\mathrm{c}}}^3} \qquad \textit{Eq. 10}$$

Inserting the relations for the particle deposition rate (Eq. 9) and the number of collectors in the packed bed element (Eq. 10) into Eq. 7 gives a well-proven expression for the sink term:

$$\sigma_{\mathrm{PB}} = \frac{3}{2} \cdot \frac{(1-\varepsilon)}{\varepsilon} \cdot \frac{\alpha \cdot \eta}{d_{\mathrm{c}}} \cdot \phi \cdot \Delta x \qquad \textit{Eq. 11}$$

The equation that results from inserting the derived sink term (Eq. 11) into the balance equation for the particle flow through the considered element (Eq. 6) can thus be expressed in the following form:

$$\frac{\phi|_{\mathrm{x}+\Delta\mathrm{x}} - \phi|_{\mathrm{x}}}{\Delta x} = -\frac{3}{2} \cdot \frac{(1-\varepsilon)}{\varepsilon} \cdot \frac{\alpha \cdot \eta}{d_{\mathrm{c}}} \cdot \phi \qquad \textit{Eq. 12}$$

The limit of the difference quotient on the left-hand side of Eq. 12 as Δx approaches zero equals $d\phi/dx$. The resulting ordinary differential equation can be solved by the separation of variables and the subsequent integration over the filter thickness, w. This assumes that the composition of the packed bed is constant across its thickness. As a result, an equation for the ratio of the particle flows leaving and entering the packed bed is obtained:

$$\frac{\phi_{\mathrm{out}}}{\phi_{\mathrm{in}}} = \exp\left[-\frac{3}{2} \cdot \frac{(1-\varepsilon) \cdot w}{\varepsilon} \cdot \frac{\alpha \cdot \eta}{d_{\mathrm{c}}}\right] \qquad \textit{Eq. 13}$$

By inserting Eq. 13 into the definition of the filtration efficiency (Eq. 5), an equation is obtained that relates the filtration efficiency of a monodisperse packed bed to the filtration properties of its collectors, specified in the form of the single-collector efficiency, $\eta = \eta\left(d_{\mathrm{c}}, d_{\mathrm{p}}\right)$, through:

$$E_{\mathrm{mono}} = 1 - \exp\left[-\frac{3}{2} \cdot \frac{(1-\varepsilon) \cdot w}{\varepsilon} \cdot \frac{\alpha \cdot \eta}{d_{\mathrm{c}}}\right] \qquad \textit{Eq. 14}$$

Assuming that all particles that come into contact with a collector adhere to it and that there is no subsequent re-entrainment (i.e., $\alpha = 1$), this derivation leads to the previously reported Eq. 2. This assumption is frequently made as adhesive forces (i.e., Van der Waals force, electrostatic force, and surface tension force due to thin liquid films) dominate by orders of magnitude other common forces involved in particle detachment (e.g., gravity, hydrodynamic, impaction, or bouncing forces) for submicron aerosol particles under typical conditions for particulate filters (Hinds, 1999). However, there are also some indications in the literature that the sticking coefficient may differ significantly from unity for particulate filters (Serrano, 2016). The validity of the predicted exponential relation between filtration efficiency and bed thickness has been confirmed experimentally by Otani et al., for instance. (Otani, 1989)

2.2 Generalized Packed Bed Filtration Model

The previously derived equation holds only for monodisperse packed beds. Of course, it is conceivable that the classical monodisperse filtration model can be extended to polydisperse packed beds using an equivalent collector diameter, d_c^eq , that characterizes the ensemble of polydisperse single-collector bodies, such that $d_\mathrm{c} = d_\mathrm{c}^\mathrm{eq}$ and $\eta = \eta\left(d_\mathrm{c}^\mathrm{eq}\right)$. As an equivalent diameter, for example, the square root mean diameter $d_c^{sq} = (\sum_i pdf(d_{\mathrm{c}i}) \cdot {d_{\mathrm{c}i}}^2)^{1/2}$ or its cubic root counterpart $d_c^{cub} = (\sum_i pdf(d_{\mathrm{c}i}) \cdot {d_{\mathrm{c}i}}^3)^{1/3}$ can be chosen.

$$E_\mathrm{class} = 1 - \exp\left[-\frac{3}{2} \cdot \frac{(1-\varepsilon) \cdot w}{\varepsilon} \cdot \frac{\alpha \cdot \eta\left(d_\mathrm{c}^\mathrm{eq}\right)}{d_\mathrm{c}^\mathrm{eq}}\right] \qquad \textit{Eq. 15}$$

To actually generalize the classical packed bed filtration model to polydisperse packed beds, however, the sink term needs to be adapted, taking into account the fact that polydisperse packed beds are composed of collectors of various diameters. The number of collectors per diameter corresponds to the product of the total number of collectors in the control volume and the number-based collector diameter probability distribution, $N_\mathrm{SC} \cdot pdf(d_{\mathrm{c}i})$. Consequently, the rate at which particles adhere to collectors of diameter d_{ci} is obtained by multiplication with the diameter-dependent deposition rate, $N_\mathrm{SC} \cdot pdf(d_{\mathrm{c}i}) \cdot \sigma_\mathrm{SC}(d_{\mathrm{c}i})$. The sink term, indicating the rate at which particles are trapped within the element, is equal to the rate at which particles are captured by all the collectors in the element and can thus be defined as follows:

$$\sigma_\mathrm{PB} = N_\mathrm{SC} \cdot \sum_i pdf(d_{\mathrm{c}i}) \cdot \sigma_\mathrm{SC}(d_{\mathrm{c}i}) \qquad \textit{Eq. 16}$$

The total number of collector spheres in the considered filter control volume, N_{SC}, also depends on the collector size distribution. As for a monodisperse bed, it can be determined by considering that the solid fraction of the packed bed is entirely constituted by the collectors:

$$N_\mathrm{SC} = \frac{6 \cdot (1-\varepsilon)}{\pi \cdot \sum_i pdf(d_{\mathrm{c}i}) \cdot {d_{\mathrm{c}i}}^3} \cdot A \cdot \Delta x \qquad \textit{Eq. 17}$$

Since the collector bodies are distributed randomly in the packed bed, no systematic dependence of the flow velocity and hence the particle flux on the collector diameter is expected. This perception of the flow within polydisperse packed beds is a key difference with the model of Wang et al., which rests on the assumption of diameter-dependent velocity fields around single-collector bodies. The diameter-dependent rate at which

particles adhere to a single-collector, $\sigma_{\mathrm{SC}}(d_{\mathrm{c}})$, is thus given by Eq. 9. Inserting it into the sink term (Eq. 16) together with the total number of collectors in the control volume (Eq. 17) yields the following relation:

$$\sigma_{\mathrm{PB}} = \frac{3(1-\varepsilon)}{2\cdot\varepsilon}\cdot\frac{\sum_i pdf(d_{\mathrm{c}i})\cdot\alpha\cdot\eta(d_{\mathrm{c}i})\cdot {d_{\mathrm{c}i}}^2}{\sum_i pdf(d_{\mathrm{c}i})\cdot {d_{\mathrm{c}i}}^3}\cdot\phi\cdot\Delta x \qquad \textit{Eq. 18}$$

In order to achieve a more concise notation, the cube root mean collector diameter, $d_{\mathrm{c}}^{\mathrm{cub}}$, is introduced. It corresponds to the diameter of a sphere having the average volume of the collectors that the polydisperse packed bed considered consists of and is thus written as follows:

$$d_{\mathrm{c}}^{cub} = \left(\sum_i pdf(d_{\mathrm{c}i})\cdot {d_{\mathrm{c}i}}^3\right)^{1/3} \qquad \textit{Eq. 19}$$

Moreover, an effective single-collector efficiency $\eta_{\mathrm{eff}} = \eta_{\mathrm{eff}}(d_{\mathrm{p}}, pdf(d_{\mathrm{c}}))$ can be defined by:

$$\eta_{\mathrm{eff}} = \frac{\sum_i pdf(d_{\mathrm{c}i})\cdot\eta(d_{\mathrm{c}i})\cdot {d_{\mathrm{c}i}}^2}{(d_{\mathrm{c}}^{cub})^2} \qquad \textit{Eq. 20}$$

It characterizes the filtration performance of the ensemble of polydisperse collectors that make up the packed bed. With these two definitions, the structure of the sink term characterizing filtration performance in polydisperse packed beds can be written similarly to that for monodisperse beds (Eq. 11) as:

$$\sigma_{\mathrm{PB}} = -\frac{3}{2}\cdot\frac{(1-\varepsilon)}{\varepsilon}\cdot\frac{\alpha\cdot\eta_{\mathrm{eff}}}{d_{\mathrm{c}}^{cub}}\cdot\phi\cdot\Delta x \qquad \textit{Eq. 21}$$

This equation is identical to Eq. 18. It is interesting to note that, in the limiting case of a monodisperse collector size distribution, Eq. 21 exactly recovers Eq. 11, which demonstrates the general nature of the proposed expression. Based on Eq. 21, a generalized equation for the filtration efficiency of any given polydisperse packed bed can then be determined using a derivation similar to that carried out for monodisperse packed beds in Section 2.1. In this way, the following expression for the filtration efficiency of polydisperse packed beds is obtained:

$$E_{\mathrm{gen}} = 1 - \exp\left(-\frac{3}{2}\cdot\frac{(1-\varepsilon)\cdot w}{\varepsilon}\cdot\frac{\alpha\cdot\eta_{\mathrm{eff}}}{d_{\mathrm{c}}^{cub}}\right) \qquad \textit{Eq. 22}$$

The above equation relates the filtration efficiency of a polydisperse packed bed to the diameter-dependent single-collector efficiencies $\eta(d_{\mathrm{c}})$ of the collectors in the bed. This model will be hereafter referred to as the generalized filtration model.

The generalized filtration model not only makes it possible to compute the overall filtration performance of polydisperse packed beds, but it also provides information on how the deposited particles are distributed among the surfaces of the different types of collectors. The contribution of individual collector types to the filtration performance of the packed bed as a whole can be quantified in this way, providing further insights into how the composition of packed beds affects their filtration characteristics. A better understanding of the influence of the composition of packed beds on their filtration performance may make it possible to draw conclusions that are also valid for porous walls and that promote the further development of particulate filters. This information is also a prerequisite for future investigations of transient filtration processes in polydisperse packed beds.

The rate at which particles adhere to all collectors of a specific diameter is $N_{\mathrm{SC}} \cdot pdf(d_{\mathrm{c}}) \cdot \sigma_{\mathrm{SC}}(d_{\mathrm{c}})$. If this rate is set in relation to the particles trapped by all collectors per unit time (Eq. 16), the fraction of particles deposited on collectors of a specific diameter, $\chi(d_{\mathrm{c}})$, is obtained through:

$$\chi(d_{\mathrm{c}i}) = \frac{pdf(d_{\mathrm{c}i}) \cdot \sigma_{\mathrm{SC}}(d_{\mathrm{c}i})}{\sum_i pdf(d_{\mathrm{c}i}) \cdot \sigma_{\mathrm{SC}}(d_{\mathrm{c}i})} \qquad \textit{Eq. 23}$$

Inserting Eq. 9 yields an expression for $\chi(d_{\mathrm{c}})$ that only depends on the composition of the packed bed being examined and the single-collector efficiency for a given collector size such that:

$$\chi(d_{\mathrm{c}i}) = \frac{pdf(d_{\mathrm{c}i}) \cdot \eta(d_{\mathrm{c}i}) \cdot {d_{\mathrm{c}i}}^2}{\sum_{d_{\mathrm{c}}} pdf(d_{\mathrm{c}i}) \cdot \eta(d_{\mathrm{c}i}) \cdot {d_{\mathrm{c}i}}^2} \qquad \textit{Eq. 24}$$

2.3 Single-collector Efficiency

All the previously and newly developed models are in fact extensions of the single-collector theory in the sense that they all rely on evaluating the efficiency of single isolated collectors. By definition, the single-collector efficiency η indicates the fraction of particles approaching a single-collector body that is actually deposited on its surface. Multiple filtration mechanisms contribute to the removal of suspended particles from the gas flow and hence must be considered when modelling single-collector efficiency. Under typical particulate filter operating conditions, filtration is governed by three mechanisms: Brownian diffusion, interception, and inertial deposition. (Joshi, 2018) Readers interested in the underlying physics are referred to a concise overview of the topic by Hinds. (Hinds, 1999) Single-collector efficiency can be computed by superposing the contributions of all relevant filtration mechanisms. (Gutfinger, 1979) For each mechanism, numerous correlations have been elaborated over the years on the basis of analytical, numerical, and experimental investigations (Gutfinger, 1979; Lee, 1979; Otani, 1989; Spurny, 1998; Long, 2009), but their respective range and degree of validity remain debatable.

3 Comparison Methodology

As discussed in the previous sections, four models can be used to extend the classical packed bed filtration model in order to predict the filtration performance of polydisperse packed beds, namely:

1) Gong et al.'s model (Eq. 1),
2) Wang et al.'s model (Eq. 4),
3) The generalized filtration model developed in Section 2.2 (Eq. 22), and
4) The extended classical filtration model (Eq. 15) using either d_c^{sq} or d_c^{cub} as equivalent diameter.

Their predictions can be compared to experimental data to assess their suitability. However, as the validity and thus the choice of the numerous analytical and empirical correlations for single-collector efficiency could skew such a comparison, the theoretical models were compared to numerical simulations performed using the commercial software GeoDict®. For this purpose, flow simulations through two polydisperse packed beds composed of quaternary and hexanary collector size distributions were conducted, and the results were compared to the predictions of the four filtration models. To circumvent problems related to the choice of

correlations for single-collector efficiency and related potential calibrations (such as those performed in the work of Gong et al. and Wang et al.), the single-collector efficiencies used were evaluated using a consistent set of additional simulations. The intention of the comparison was to determine the most accurate theoretical approach among the four available models in order to extend the single-collector theory to polydisperse packed beds.

3.1 Simulation Details

The numerical simulations were performed using the FilterDict module of the commercial software GeoDict® (GeoDict, 2020), which proved to be a reliable solution for computing the flow field and filtration performance of filter structures. (Gervais, 2015; Azimian, 2017; Belot, 2020) To obtain the flow field by solving the steady-state Stokes equation, the LIR solver (a very fast and memory efficient iterative finite volume solver using an LIR-tree for spatial partitioning) was used on structured Cartesian grids that discretized the packed bed structures being investigated and on which the fluid and solid phases were encoded in a Boolean manner. Based on the computed flow field, the trajectory and eventual capture of particles of various sizes transported by the exhaust gas (here assumed to be air) were computed by solving a stochastic Langevin problem using FilterDict. The procedure assumed that the soot concentration was low so that the flow disturbance caused by the motion of aerosol particles was negligible and that particles adhered to a collector on first contact with its surface without re-entrainment being possible, corresponding to a sticking coefficient of $\alpha = 1$. Furthermore, in accordance with the assumptions on which the analytical models are based, the accumulation of particles on the collector bodies and the resulting clogging of the filter are not considered. Table 1 summarizes the physical and simulation parameters used for the two polydisperse packed beds investigated. The process conditions chosen for the simulations were typical for particulate filters and, under these conditions, the re-entrainment of particles due to hydrodynamic forces or impaction forces from incoming particles is unlikely as Reynolds (Re) and Stokes (St) numbers are well below the respective threshold values (i.e., $Re \gg 1$ and $St > 0.81^2$) reported by Hinds for its occurrence (Hinds, 1999).

Table 1: Various parameters used for the simulations for the two polydisperse packed beds investigated.

Physical Parameters			
Parameter	Symbol	Value	
		Quaternary packed bed	Hexanary packed bed
Particle density [kg/m³]	ρ_{p}	800	800
Gas density [kg/m³]	ρ_{g}	1.177	0.588
Gas viscosity [Pa·s]	μ_{g}	$1.858 \cdot 10^{-5}$	$3.017 \cdot 10^{-5}$
Free mean path [m]	λ_{g}	$6.880 \cdot 10^{-8}$	$1.605 \cdot 10^{-7}$
Superficial velocity [mm/s]	$\bar{U}$	80	20
Temperature [K]	T	300	600
Bed porosity [%]	ϵ	68.5	60.0
Evaluated bed thickness [µm]	w	250.0	304.8
Domain lateral dimensions [µm]	-	600.6	311.5
Number-based collector size distribution	pdf	See Figure 3	See Figure 4
Total number of collectors [-]	N_{SC}	37644	4247
Cube root mean collector diameter [µm]	d_{c}^{cub}	12.2	19.2
Square root mean collector diameter [µm]	d_{c}^{sq}	11.2	18.6
Aerosol particle sizes [µm]	d_{p}	$0.01\ \mu\mathrm{m} \leq d_p \leq 1\ \mu\mathrm{m}$	$0.01\ \mu\mathrm{m} \leq d_p \leq 1\ \mu m$
Simulation Parameters			
Parameter	Symbol	Value	
		Quaternary packed bed	Hexanary packed bed
Grid spacing [µm]	Δx	1.246	1.246
Convergence criterion	-	0.001	0.001
Lateral boundary condition	-	periodic	symmetric
Inlet/outlet boundary condition	-	VinPout[1]	VinPout[1]
Number of particles tracked [-]	-	250,000	100,000

[1] Constant inlet velocity and constant outlet pressure.

Figure 3 and Figure 4 present the two packed beds and their corresponding collector size distributions, which are quaternary and hexanary, respectively. While the composition of the quaternary packed bed was chosen such that the predictions of the analytical models being compared differed distinctly, the hexanary packed bed exhibited characteristics that made it comparable to packed beds used as a surrogate model for particulate filters, with collector diameters ranging from 10 µm to 35 µm whose relative abundance was taken from a lognormal distribution. To ensure that the computed filtration properties did not depend on the random arrangement of the collectors in the packed bed, the structures considered for the simulations were taken to be large enough to constitute a representative elementary volume. Similarly, the number of aerosol particle trajectories computed were sufficiently large (> 100,000) so that statistical variability had very little to no impact on the filtration performance computed.

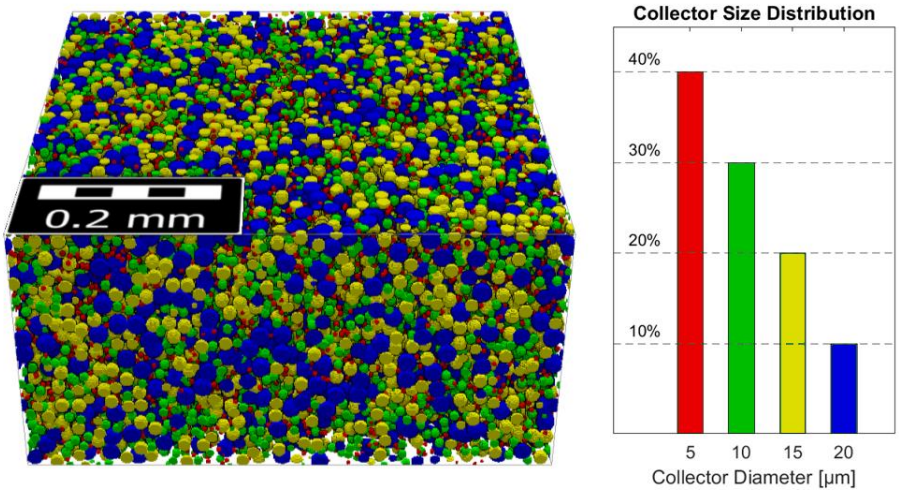

Figure 3: Visualization and composition of the quaternary packed bed.

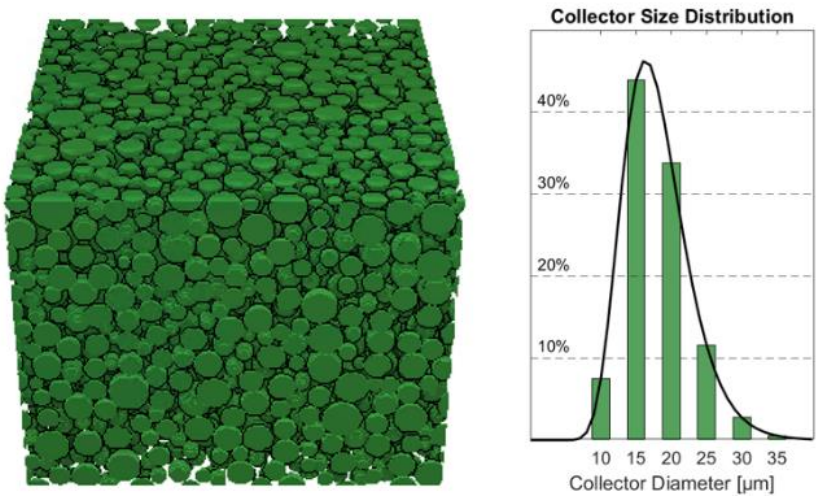

Figure 4: Visualization and composition of the hexanary packed bed.

Based on the computed particle trajectories, the filtration performance of the packed beds was evaluated. When a particle-laden gas flows through a packed bed, the number of suspended particles decreases each time a tracked particle comes into contact with a collector. From the computed contact positions, the decrease in the

number of suspended particles, Φ, with increasing filter thickness passed, x, can be determined. A typical result is plotted schematically in Figure 5. It can be seen that, inside the packed bed, the number of suspended particles decreases exponentially with the thickness of the bed. It is also apparent that disturbances occur when the particle-laden flow enters and exits the packed bed. To avoid distortions, inflow and outflow regions were excluded from the analysis at both ends of the packed bed and only the bulk region was considered. Accordingly, the structures used for the simulations were extended such that the desired thickness w remained after the removal of the inlet and outlet regions.

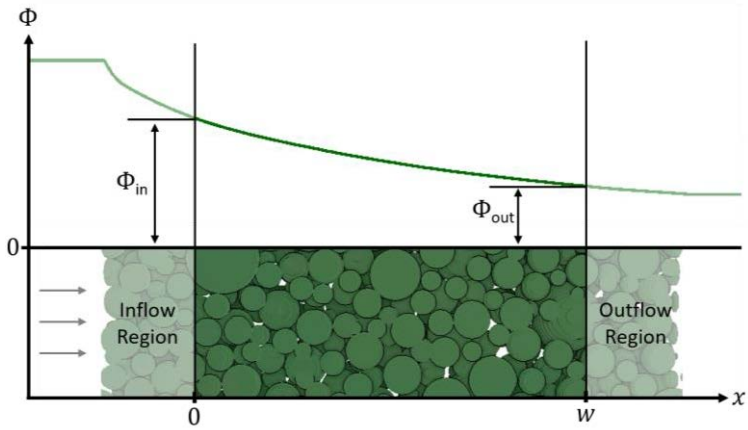

Figure 5: Schematic of typical variations in the number of suspended particles (Φ) with increasing packed bed thickness (x).

The information obtained on the number of suspended particles over filter thickness served as basis for the evaluation of filtration efficiency, which can be computed from the number of particles leaving and entering the section analyzed using the following simple equation: $E = 1 - \Phi_{\text{out}}/\Phi_{\text{in}}$.

3.2 Calculation of Single-collector Efficiency

As mentioned earlier, all four theoretical models rely on the evaluation of single-collector efficiencies of the differently sized collector bodies contained in the polydisperse packed bed whose filtration performance was to be predicted. To ensure comparability with the numerical simulations, the single-collector efficiencies used to feed the analytical models are determined from consistent simulations. A suitable method to calculate the single-collector efficiency from simulations of the filtration performance of monodisperse packed beds is proposed in this section.

Based on the classical filtration theory, it is known that the number of suspended particles in monodisperse packed beds decreases exponentially with the thickness passed, x, such that:

$$\Phi(x) = \Phi_{\text{in}} \cdot e^{-\lambda \cdot x} \qquad \textit{Eq. 25}$$

In Eq. 25, the coefficient λ in the exponent is related to single-collector efficiency through:

$$\lambda = \frac{3}{2} \cdot \frac{(1-\varepsilon)}{\varepsilon} \cdot \frac{\eta}{d_{\text{c}}} \qquad \textit{Eq. 26}$$

The single-collector efficiencies of any collector under given process conditions can thus be computed if λ can be determined through a linear regression of $\ln(\Phi)$ as a function of the spatial coordinate x in the bulk of the filter,

with -λ being the slope of the resulting line, as illustrated for an actual monodisperse case in Figure 6. The high R^2 value reported for the regression in the example of Figure 4, as well as the high mean coefficient of determination obtained for all regressions performed ($\overline{R^2} > 0.998$), validated the soundness of the proposed approach to determine single-collector efficiencies.

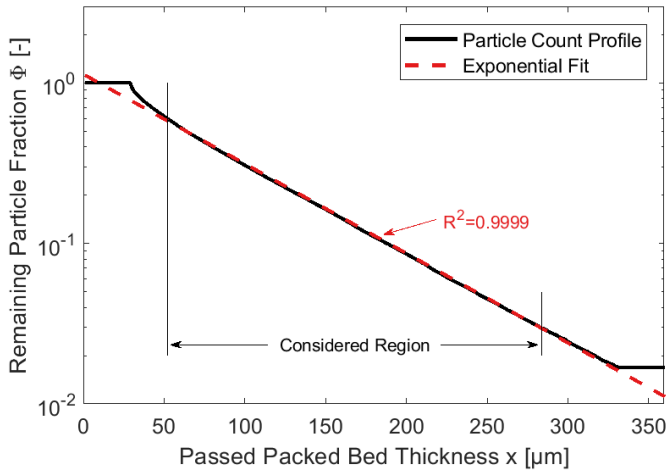

Figure 6: Example of an exponential fit to determine single-collector efficiency from simulation data for a monodisperse packed bed.

As such, the consistent single-collector efficiencies required can be evaluated from simulations with monodisperse structures. It is important, however, that they be performed with the same porosity, operating conditions, and grid spacing as the polydisperse packed bed being considered. As single-collector efficiency depends on flow velocity and as the analytical filtration models considered here are based on different assumptions about the velocity fields in polydisperse packed beds, independent data sets of single-collector efficiencies had to be generated for the different models. One representative set of resulting single-collector efficiencies obtained from the proposed procedure is shown in Figure 7.

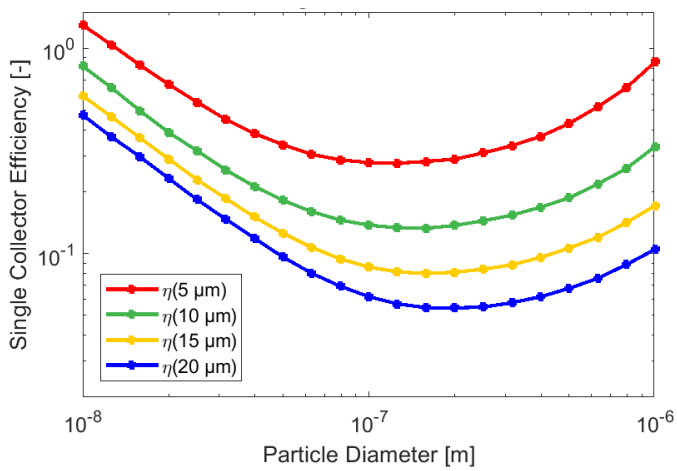

Figure 7: Single-collector efficiencies as a function particle diameter determined from monodisperse packed bed simulations and used for the prediction of the generalized model for the filtration performance of the quaternary packed bed.

One point worth mentioning as it has never been documented before to the authors' knowledge is that the capture efficiency computed using the reported simulation approach converged very weakly as the grid spacing was decreased. As such, satisfactorily converged capture efficiencies (e.g., with variations lower than 1-2% as the grid is further refined by a factor of two) could not be reached with practical grids. This finding indicates that the

filtration properties of the resulting voxelized collectors deviated significantly from those of smooth spheres because they were not discretized finely enough. This convergence behavior was observed not only with FilterDict's Langevin solver, but with another Langevin solver used in previous studies (Rebaï, 2011; Matte-Deschênes, 2016), as well. As a result, the capture efficiency reported at a relatively coarse grid spacing must be considered as that of "rough" collectors. Despite this restriction, the comparison of the simulation and theoretical model predictions remains valid as all the approaches were compared on the same basis, i.e., with collectors with the same given roughness, as the polydisperse simulations used for the comparison and the monodisperse simulations used to feed the theoretical filtration models with consistent single-collector efficiencies were all performed with the same grid spacing.

4 Results and Discussion

Figure 8 presents the computed filtration efficiencies for the quaternary packed bed as a function of aerosol particle diameter using the four theoretical polydisperse models (colored lines) and GeoDict® numerical simulations (black squares). The computed predictions of the filtration models rest on individual sets of single-collector efficiencies determined at different velocities, reflecting the divergent perceptions of the flow field within polydisperse packed beds on which the different models were derived. Although all the curves obtained for filtration efficiency have the typical smile-like shape, with a minimum at particle diameters in the order of $100 - 200\,\mathrm{nm}$, they differ considerably quantitatively. The predictions of the generalized filtration model were in excellent agreement with the results from the numerical simulations. The extended classical filtration model, in contrast, systematically overestimated filtration performance, while the values determined on the basis of the cube root mean diameter are, however, clearly in better agreement with the simulation results than those obtained using the square mean root diameter. The other two polydisperse filtration models, i.e., the models by Gong et al. and Wang et al., strongly underestimated it. The good agreement between the proposed generalized filtration model and the numerical simulations also became evident when comparing its predictions for the decrease of suspended particles within the packed bed, which are shown in Figure 9.

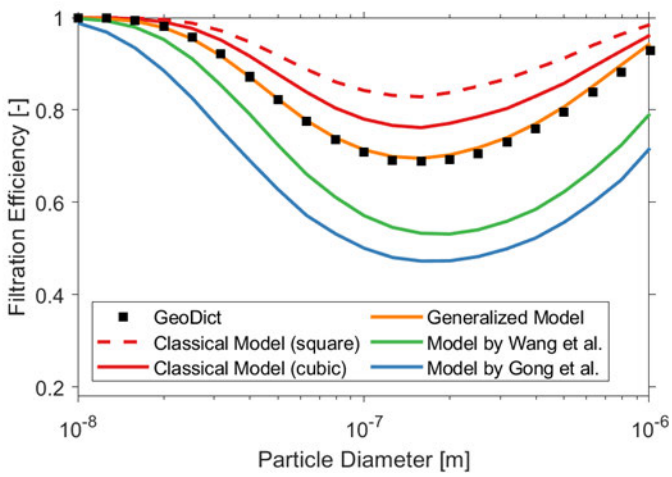

Figure 8: Comparison of the filtration efficiency predictions for the quaternary packed bed obtained with the four theoretical polydisperse filtration models and with GeoDict® simulations. Square and cubic refer respectively to the square root and cubic root mean diameters used as equivalent diameter in the extended classical filtration theory (Eq. 15).

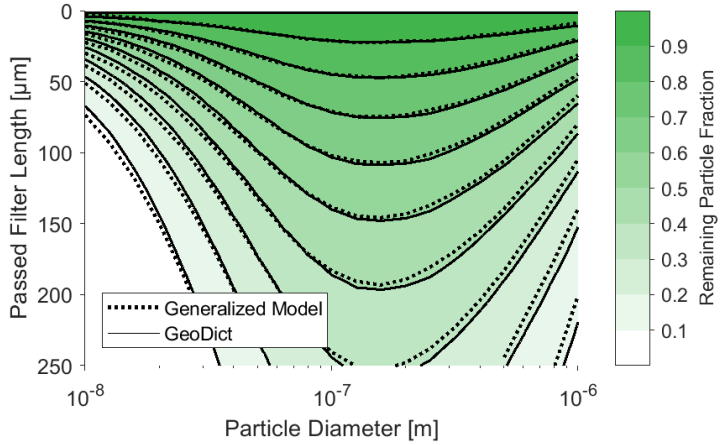

Figure 9: Remaining fraction of suspended particles in the packed bed as a function of their diameter as predicted by the generalized model compared to the GeoDict® numerical results.

Figure 10 presents the same comparison as in Figure 8 but for the hexanary packed bed. Similar conclusions can be drawn. The extended classical filtration model slightly overestimated the filtration efficiency of the polydisperse packed bed, while the models by Gong et al. and Wang et al. tended to underestimate it. The prediction of the generalized model, on the other hand, was in fairly good agreement with the numerical simulation results across all particle diameters, although the agreement was slightly lower than for the quaternary packed bed.

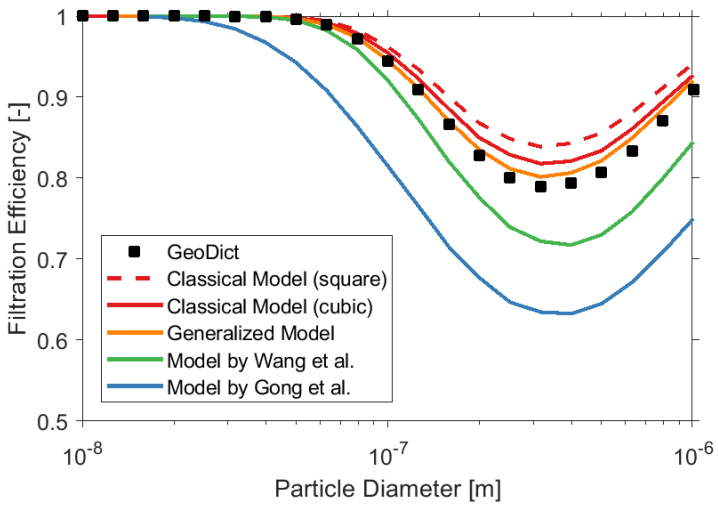

Figure 10: Comparison of the filtration efficiency predictions for the hexanary packed bed obtained with the four theoretical polydisperse filtration models and with the GeoDict® simulations. Square and cubic refer respectively to the square root and cubic root mean diameters used as equivalent diameter in the extended classical filtration theory (Eq. 15).

It is apparent that the predicted filtration efficiencies for particles with diameters greater than $\sim 200\,nm$ were marginally higher than those from the simulations. One possible explanation for this effect is that the single-collector efficiencies used to compute the analytical predictions were determined from simulations with monodisperse packed beds. Unlike in polydisperse beds, the collectors here were surrounded only by collector bodies of the same diameter. Neighboring collectors, however, mutually influence each other in their filtration

properties. Thus, it cannot be presumed that a collector body in a monodisperse packed bed has identical filtration properties as in a polydisperse bed of the same packing density in which it is surrounded by collectors of various diameters. In general, the mutual influence of the collectors has a much stronger effect on the filtration mechanism of interception than on that of Brownian diffusion. (Gutfinger, 1979) It is thus probable that the associated deviations are more pronounced for particles for which interception is the dominant filtration mechanism. Furthermore, the suspected effect might explain the fact that the deviations were significantly smaller for the first packed bed investigated. As it had a lower packing density, interactions between the collectors generally affected its filtration characteristics less.

Despite these minor discrepancies for larger particle diameters, the presented data show that the predictions of the generalized packed bed filtration model (i.e., Eq. 22 combined with Eq. 19 and Eq. 20) for the overall filtration performance of the polydisperse packed beds investigated were in excellent agreement with the simulations. It consistently outperformed all the other theoretical filtration models in predicting the simulation results. The extended classical filtration model using the cube root mean diameter as an equivalent monodisperse diameter was the second-best model (Eq. 14) but had a tendency to overestimate filtration efficiency. However, since it used a monodisperse packed bed as a surrogate model for polydisperse packed beds, it could not provide any information on the influence of the inhomogeneous microstructure of polydisperse packed beds on their filtration performance. The generalized model, on the other hand, was able to deliver additional insights into the relative contribution of individual collector bodies to the overall filtration properties as a more detailed comparison of the predictions from the generalized filtration model with the simulation results for the quaternary packed bed structure reveals.

As the filtration effect of a packed bed is due to the deposition of suspended particles on the surfaces of its collectors, it is essential that a suitable filtration model be not only capable of computing the overall filtration performance of packed beds but also provide accurate predictions for the contribution of individual collector types to the capture of particles. Figure 11 presents these predictions of the generalized filtration model (using Eq. 19) and compares them to those of the GeoDict® simulations. In general, the predictions and simulations for the relative contributions of the four collector types to capture as a function of particle size followed fairly similar trends. As already discussed for filtration efficiency, the deviations increased notably with increasing particle diameter, which again could be due to the single-collector efficiencies used that were susceptible to be interfered with in the interception-dominated regime (i.e., at particle sizes greater than 100-200 nm). However, the contributions of collectors smaller than the cube root mean collector diameter ($12.2\,\mu m$) were systematically slightly overestimated, even for small particle diameters, while those of larger collectors were obviously underestimated. Nevertheless, with an average relative error of 12.8% compared to the simulations, the predictions of the generalized filtration model were in significantly better agreement than those of the models of Gong et al. and Wang et al., with relative errors of 83.5% and 45.2%, respectively.

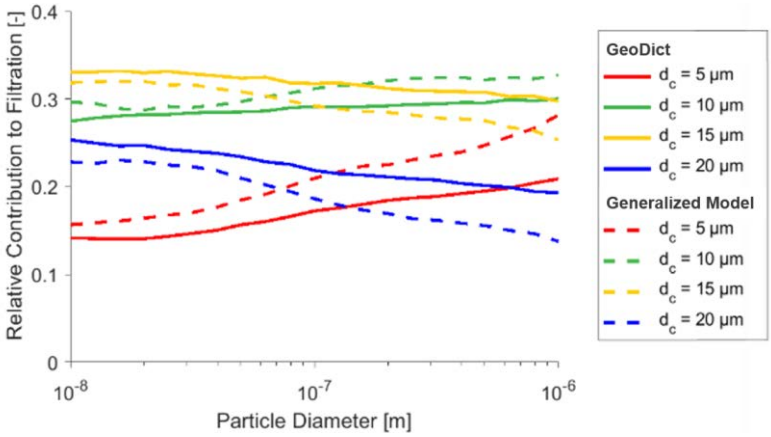

Figure 11: Relative contributions of the different collector types to the overall filtration performance of the quaternary packed bed.

5 Conclusions and Outlook

Porous filter walls such as those found in wall-flow particulate filters are highly irregular media. Surrogate structures of reduced complexity are thus necessary to model their filtration performance using analytical methods. In this context, polydisperse packed beds have recently received special attention. Compared to conventional monodisperse packed beds, they have the potential to better represent the inhomogeneity of the microstructure of porous filters. Analytical models for predicting the filtration performance of polydisperse packed beds are thus of great interest.

In the present paper, a generalized analytical filtration model for clean packed beds of any composition is introduced. The model relates the filtration performance of polydisperse packed beds to the filtration characteristics of the single-collector bodies they contain. It was derived as an extension of the well-proven classical packed bed filtration theory. The generalized filtration model makes it possible to compute the overall filtration properties of clean polydisperse packed beds as well as the respective contributions of individual collector types to their filtration performance insofar as correlations for the capture efficiency of each single-collector are available. The predictions of the newly developed model were compared to the results of numerical simulations for two polydisperse packed beds. The comparison showed that the predictions of the generalized model are in considerably better agreement with the simulations than those of previously published analytical models.

In order to most effectively apply the generalized filtration model to the field of particulate filters, future research should focus on more robust approaches than MIP to derive the composition of polydisperse packed beds that better represent the filter medium being investigated. One prospective approach would be to approximate the solid space geometry of particulate filters obtained from computed microtomography using maximally inscribed, non-overlapping polydisperse spheres (see, for example, (Fordyce, 2020)). The proposed generalized filtration model could then be integrated into extended reduced-order models to better predict, control, or optimize the behavior of particulate filters or their geometry. For instance, it is conceivable to use it to model transient filtration processes following the approach presented by Konstandopoulos et al. (Konstandopoulos, 2000) Similarly, the influence of local inhomogeneities of packed bed properties could be taken into account, as described by Gong et al. (Gong, 2015a) Lastly, it is also conceivable that the filtration model proposed in the

present paper will find applications in other engineering problems such as membrane filters, granular activated carbon filters, pressure swing adsorption systems, and granular bed filters for hot gas cleaning.

Acknowledgements

The research at TU Darmstadt was supported by the Bundesministerium für Bildung und Forschung in the framework of the project ML-MORE (05M20RDA).

References

Adam, F., Olfert, J., Wong, K.F., Kunert, S. & Richter, J.M. (2020). Effect of Engine-Out Soot Emissions and the Frequency of Regeneration on Gasoline Particulate Filter Efficiency. *SAE Technical Paper* 2020-01-1431.

Azimian, M., Cheng, L. & Wiegmann, A. (2017). Simulation of soot filtration in diesel particulate filter with GeoDict, *15th FAD-Conference, Dresden, Germany* (https://www.geodict.com/Presentations/2017FAD_Dresden_MA.pdf).

Belot, I., Vidal, D., Votsmeier, M., Hayes, R. E. & Bertrand, F. (2020). Numerical investigation of the impact of washcoat distribution on the filtration performance of gasoline particulate filters. *Chemical Engineering Science,* 221, 115656.

Belot, I., Sun, Y., Vidal, D., Votsmeier, M., Causse, P., Trochu, F., & Bertrand, F. (2021). A 3D additive manufacturing approach for the validation of a numerical wall-scale model of catalytic particulate filters. *Chemical Engineering Journal*, *405*, 126653.

Diamond, S. (2000). Mercury porosimetry: an inappropriate method for the measurement of pore size distributions in cement-based materials. *Cement and concrete research*, *30*(10), 1517-1525.

Fordyce, A. J., Knuefing, L., Ainsworth, T. D., Beeching, L., Turner, M., & Leggat, W. (2020). Understanding decay in marine calcifiers: Micro-CT analysis of skeletal structures provides insight into the impacts of a changing climate in marine ecosystems. *Methods in Ecology and Evolution*, *11*(9), 1021-1041.

GeoDict (2020), version 2020. Retrieved from www.geodict.com: Math2Market GmbH.

Gervais, P. C., Bourrous, S., Dany, F., Bouilloux, L., & Ricciardi, L. (2015). Simulations of filter media performances from microtomography-based computational domain. Experimental and analytical comparison. *Computers & Fluids*, *116*, 118-128.

Gong, J. & Rutland, C. J. (2015a). Filtration characteristics of fuel neutral particulates using a heterogeneous multiscale filtration model. *Journal of Engineering for Gas Turbines and Power,* 137(11).

Gong, J. & Rutland, C. J. (2015b). PDF-based heterogeneous multiscale filtration model. *Environmental science & technology,* 49(8), 4963-4970.

Gong, J., Stewart, M. L., Zelenyuk, A., Strzelec, A., Viswanathan, S., Rothamer, D. A., Foster, D.E. & Rutland, C. J. (2018). Importance of filter's microstructure in dynamic filtration modeling of gasoline particulate filters (GPFs): Inhomogeneous porosity and pore size distribution. *Chemical Engineering Journal*, *338*, 15-26.

Greiner, R., Prill, T., Iliev, O., van Setten, B. A., & Votsmeier, M. (2019). Tomography based simulation of reactive flow at the micro-scale: Particulate filters with wall integrated catalyst. *Chemical Engineering Journal*, *378*, 121919.

Guan, B., Zhan, R., Lin, H., & Huang, Z. (2015). Review of the state-of-the-art of exhaust particulate filter technology in internal combustion engines. *Journal of environmental management*, *154*, 225-258.

Gutfinger, C., & Tardos, G. I. (1979). Theoretical and experimental investigation on granular bed dust filters. *Atmospheric Environment (1967)*, *13*(6), 853-867.

Hinds, W. C. (1999). Aerosol technology: properties, behavior, and measurement of airborne particles. *John Wiley & Sons*, 1999.

Joshi, A., & Johnson, T. V. (2018). Gasoline particulate filters—A review. *Emission Control Science and Technology*, *4*(4), 219-239.

Koltsakis, G., Haralampous, O., Depcik, C., & Ragone, J. C. (2013). Catalyzed diesel particulate filter modeling. *Reviews in Chemical Engineering*, *29*(1), 1-61.

Konstandopoulos, A. G., & Johnson, J. H. (1989). Wall-flow diesel particulate filters—their pressure drop and collection efficiency. *SAE Transactions*, 625-647.

Konstandopoulos, A. G., Kostoglou, M., Skaperdas, E., Papaioannou, E., Zarvalis, D., & Kladopoulou, E. (2000). Fundamental studies of diesel particulate filters: transient loading, regeneration and aging. *SAE transactions*, 683-705.

Kuwabara, S. (1959). The forces experienced by randomly distributed parallel circular cylinders or spheres in a viscous flow at small Reynolds numbers. *Journal of the physical society of Japan*, *14*(4), 527-532.

Lee, K. W., & Gieseke, J. A. (1979). Collection of aerosol particles by packed beds. *Environmental Science & Technology*, *13*(4), 466-470.

Logan, B. E., Jewett, D. G., Arnold, R. G., Bouwer, E. J., & O'Melia, C. R. (1995). Clarification of clean-bed filtration models. *Journal of environmental engineering*, *121*(12), 869-873.

Long, W., & Hilpert, M. (2009). A correlation for the collector efficiency of Brownian particles in clean-bed filtration in sphere packings by a Lattice-Boltzmann method. *Environmental science & technology*, *43*(12), 4419-4424.

Matte-Deschênes, G., Vidal, D., Bertrand, F., & Hayes, R. E. (2016). Numerical investigation of the impact of thermophoresis on the capture efficiency of diesel particulate filters. *The Canadian Journal of Chemical Engineering*, *94*(2), 291-303.

Moro, F., & Böhni, H. (2002). Ink-bottle effect in mercury intrusion porosimetry of cement-based materials. *Journal of Colloid and Interface Science*, *246*(1), 135-149.

Otani, Y., Kanaoka, C., & Emi, H. (1989). Experimental study of aerosol filtration by the granular bed over a wide range of Reynolds numbers. *Aerosol science and technology*, *10*(3), 463-474.

Plachá, M., Kočí, P., Isoz, M., Svoboda, M., Price, E., Thompsett, D., Kallis, K. & Tsolakis, A. (2020). Pore-scale filtration model for coated catalytic filters in automotive exhaust gas aftertreatment. *Chemical Engineering Science*, *226*, 115854.

Rebaï, M., Drolet, F., Vidal, D., Vadeiko, I., & Bertrand, F. (2011). A Lattice Boltzmann approach for predicting the capture efficiency of random fibrous media. *Asia-Pacific Journal of Chemical Engineering*, *6*(1), 29-37.

Serrano, J. R., Climent, H., Piqueras, P., & Angiolini, E. (2016). Filtration modelling in wall-flow particulate filters of low soot penetration thickness. *Energy*, *112*, 883-898.

Spurny, K. R. (1998). Advances in aerosol gas filtration. *CRC Press*.

Viswanathan, S., Stewart, M. L., & Rothamer, D. A. (2021). Experimental Investigation of the Effect of Pore Size Distribution on Nano-particle Capture Efficiency Within Ceramic Particulate Filters. *Emission Control Science and Technology*, *7*(1), 26-40.

Votsmeier, M., Kreuzer, T., Gieshoff, J., & Lepperhoff, G. (2009). Automobile exhaust control. *Ullmann's Encyclopedia of Industrial Chemistry*, *4*, 407-424.

Walter, R., Neumann, J., & Hinrichsen, O. (2020). Extended Model for Filtration in Gasoline Particulate Filters under Practical Driving Conditions. *Environmental Science & Technology*, *54*(15), 9285-9294.

Wang, Y., Gong, J., Su, C., Ou, Q., Lyu, Q., Pui, D., & Cunningham, M. J. (2020). Theoretical Framework of a Polydisperse Cell Filtration Model. *Environmental science & technology*, *54*(18), 11230-11236.

Symbols and Abbreviations

A	Element cross-sectional area normal to flow	$[m^2]$
d_c	Collector diameter	$[m]$
d_p	Particle diameter	$[m]$
E	Filtration efficiency	$\left[\frac{mol}{mol}\right]$
N_{SC}	Total number of collectors	$[-]$
pdf	Normalized collector diameter distribution by number	$\left[\frac{mol}{mol}\right]$
PDF	Normalized collector diameter distribution by volume	$\left[\frac{m^3}{m^3}\right]$
w	Packed bed thickness	$[m]$
x	Position coordinate	$[m]$
α	Sticking coefficient	$\left[\frac{mol}{mol}\right]$
ε	Porosity	$\left[\frac{m^3}{m^3}\right]$

η	Single-collector efficiency	$\left[\frac{mol}{mol}\right]$
λ	Exponent characterizing decrease of particles	$\left[\frac{1}{m}\right]$
σ_{PB}	Particle removal rate in a packed bed element	$\left[\frac{mol}{s}\right]$
σ_{SC}	Particle deposition rate on a single-collector	$\left[\frac{mol}{s}\right]$
ϕ	Flow rate of suspended particles	$\left[\frac{mol}{s}\right]$
Φ	Number of suspended particles	$[mol]$
χ	Fraction of filtered particles trapped by a specific collector type	$\left[\frac{mol}{mol}\right]$